A Quantum Monte Carlo Approach to the Adiabatic Connection Method

Maziar Nekovee and W.M.C. Foulkes
The Blackett Laboratory, Imperial College,
Prince Consort Road, London SW7 2BZ, UK

A.J. Williamson, G. Rajagopal and R.J. Needs
TCM group, Cavendish Laboratory,
Madingley Road, Cambridge CB3 0HE, UK

Abstract

We present a new method for realizing the adiabatic connection approach in density functional theory, which is based on combining accurate variational quantum Monte Carlo calculations with a constrained optimization of the ground state many-body wavefunction for different values of the Coulomb coupling constant. We use the method to study an electron gas in the presence of a cosine-wave potential. For this system we present results for the exchange-correlation hole and exchange-correlation energy density, and compare our findings with those from the local density approximation and generalized gradient approximation.

1 Introduction

Density functional theory (DFT) (1, 2) is the main computational tool for the treatment of many-body effects in solid state electronic structure calculations and is now widely used to determine ground-state properties of atoms and molecules (3). In the Kohn-Sham formulation of DFT (2) the problem of finding the ground state energy and density of an interacting N-electron system is tranformed into an equivalent problem involving non-interacting electrons. The central quantity in this formulation is the exchange-correlation energy E_{xc}, which is a universal functional of the electron density $n(\mathbf{r})$. The exchange-correlation energy functional, a complicated many-body object, is the big unknown of the theory and the core problem in the density functional approach is to find accurate approximations for E_{xc}. The most frequently used approximations to date are the local density approximation (LDA) (2) and various generalized gradient approximations (GGA) (4, 5, 6).

An entirely different approach to the ground-state many-body problem is quantum Monte Carlo (QMC) (7). QMC calculations are computationally more demanding than density functional calculations. However, unlike the density functional approach, in which the ground-state density is the basic variable, quantum Monte Carlo methods focus on sampling the full ground-state many-body wavefunction of the system under consideration and hence yield a more detailed description of many-body effects. Quantum Monte Carlo calculations can therefore be used to investigate density functional theory from "outside" and to test the performance of approximations to E_{xc}. In the last few years a number of quantum Monte Carlo investigations of DFT have been reported for atoms and molecules (8, 9), model solids (10, 11) and silicon (12). Most of these investigations focused on extracting the exchange-correlation potential and components of exchange-correlation energy from accurate electron densities obtained from Monte Carlo calculations. Except for a very recent calculation by Hood *et al.*(12), other key quantities in DFT, namely the exchange-correlation hole n_{xc} and the exchange-correlation energy density e_{xc}, have not been investigated with Monte Carlo methods. These quantities, however, are important in understanding the success of the LDA beyond its formal limits of validity, and play a key role in constructing more accurate approximations to E_{xc}. A better knowledge of these quantities is therefore crucial for a better understanding of the performance of the LDA and various corrections to it such as GGAs, and can guide the construction of more accurate functionals. Unlike V_{xc} which can be directly obtained from the electron density (by inversion of the Kohn-Sham equations (10, 8)) evaluating e_{xc} and n_{xc} is more demanding. These quantities are derived from an adiabatic connection procedure in which one scales the Coulomb interaction by a factor λ

while keeping the density fixed at the ground state density of the system under consideration. To extract n_{xc} and e_{xc} from Monte Carlo data one therfore needs to calculate not only the ground state many-body wavefunction of the fully interacting system ($\lambda = 1$), but also the many-body wavefunction in the range $0 \leq \lambda < 1$.

Within variational quantum Monte Carlo, we have developed a new scheme for realizing the above adiabatic connection procedure which allows us to extract n_{xc} and ϵ_{xc} from Monte Carlo data. Our method is based on a constrained optimization of the many-body wavefunction at different Coulomb coupling constants using the technique of variance minimization (13, 14). In this paper we will discuss aspects of our method and illustrate it with a first application to an electron gas exposed to a cosine-wave potential. For this system we calculate the exchange-correlation energy, exchange-correlation energy density and exchange-correlation hole, and compare our findings with those obtained from the LDA and the most commonly used version of GGA (6, 15).

2 The Adiabatic Connection

The idea of an adiabatic connection to determine E_{xc} has been developed by several authors (16-18). Here we closely follow the review by Parr and Yang (3). We consider a system of N interacting electrons in the presence of an external potential $V_{ex}(\mathbf{r})$ and characterized by the Hamiltonian (atomic units are used throughout, with $e = \hbar = m = 1$)

$$\hat{H} = \hat{T} + \hat{V}_{ee} + \hat{V}_{ex} \tag{1}$$

with

$$\hat{T} = \sum_{i=1}^{N} -\frac{1}{2}\nabla_i^2 \tag{2}$$

$$\hat{V}_{ee} = \frac{1}{2}\sum_{i=1}^{N}\sum_{j\neq i}^{N}\frac{1}{|\mathbf{r}_i - \mathbf{r}_j|} \tag{3}$$

$$\hat{V}_{ex} = \sum_{i=1}^{N} V_{ex}(\mathbf{r}_i) \tag{4}$$

In the Kohn-Sham formulation of DFT the problem of finding the ground state energy of this system is exactly mapped onto one of finding the electron density which minimizes the total energy functional

$$E[n(\mathbf{r})] = T_0[n(\mathbf{r})] + E_H[n(\mathbf{r})] + \int d\mathbf{r} V_{ex}(\mathbf{r})n(\mathbf{r}) + E_{xc}[n(\mathbf{r})] \tag{5}$$

Here T_0 is the kinetic energy of a fictitious non-interacting system of N electrons having the same electron density $n(\mathbf{r})$ as the interacting system and $E_H[n]$ is the Hartree (electrostatic) energy. The exchange-correlation energy functional $E_{xc}[n]$ is usually defined by equation (5) and contains all the many-body terms not considered elsewhere in (5).

An exact expression for E_{xc} is obtained by scaling the electron-electron interaction with a factor λ and varying λ between 1 (real system) and 0 (non-interacting system). The exchange-correlation functional E_{xc} is then given by (3)

$$E_{xc}[n] = \int_0^1 d\lambda < \Psi^\lambda | \hat{V}_{ee} | \Psi^\lambda > - E_H[n] \tag{6}$$

where Ψ^λ is the anti-symmetric many-body wavefunction which minimizes

$$F^\lambda =< \hat{T} + \lambda \hat{V}_{ee} > \tag{7}$$

under the fixed-density constraint

$$< \Psi^\lambda | \hat{n}(\mathbf{r}) | \Psi^\lambda >= n(\mathbf{r}) \tag{8}$$

and $\hat{n}(\mathbf{r})$ is the density operator

$$\hat{n}(\mathbf{r}) = \sum_{i=1}^{N} \delta(\mathbf{r} - \mathbf{r}_i). \tag{9}$$

A minimum for F^λ always exists (20) and, except under some unusual conditions (21), Ψ^λ can be obtained from the following Schrödinger equation

$$[\hat{T} + \lambda \hat{V}_{ee} + \hat{V}^\lambda] \Psi^\lambda = \hat{H}_\lambda \Psi_\lambda = E^\lambda \Psi^\lambda \tag{10}$$

with

$$\hat{V}^\lambda = \sum_{i=1}^{N} V^\lambda(\mathbf{r}_i). \tag{11}$$

The potential $V^\lambda(\mathbf{r})$ at point $\mathbf{r}$ is a Lagrange multiplier corresponding to the fixed-density constraint at that point. As λ varies between 0 and 1, $V^\lambda(\mathbf{r})$ must be adjusted such that the electron density remains fixed at $n(\mathbf{r})$. At $\lambda = 1$, V^λ coincides with the actual external potential $V_{ex}(\mathbf{r})$ while at $\lambda = 0$, it coincides with the Kohn-Sham effective potential,

$$V^{\lambda=0}(\mathbf{r}) = V_{eff}(\mathbf{r}) = V_{ex}(\mathbf{r}) + V_H(\mathbf{r}) + V_{xc}(\mathbf{r}) \tag{12}$$

where V_H is the Hartree (electrostatic) potential

$$V_H(\mathbf{r}) = \int d\mathbf{r}' \frac{n(\mathbf{r}')}{|\mathbf{r} - \mathbf{r}'|} \tag{13}$$

and

$$V_{xc}(\mathbf{r}) = \frac{\delta E_{xc}[n]}{\delta n(\mathbf{r})} \tag{14}$$

is the Kohn-Sham exchange-correlation potential. Note also that $\Psi^{\lambda=0}$ corresponds to the Slater determinant of the exact Kohn-Sham orbitals corresponding to the density $n(\mathbf{r})$.

The adiabatic expression (6) allows us to obtain several useful decompositions of E_{xc}. Inserting (3) in (6) gives

$$E_{xc}[n(\mathbf{r})] = \frac{1}{2}\int d\mathbf{r} \int d\mathbf{r}' \; \frac{n(\mathbf{r}) n_{xc}(\mathbf{r}, \mathbf{r}')}{|\mathbf{r} - \mathbf{r}'|} \tag{15}$$

where n_{xc} is the density-functional exchange-correlation hole defined by (3)

$$\bar{n}(\mathbf{r}, \mathbf{r}') = n(\mathbf{r}) n(\mathbf{r}') + n(\mathbf{r}) n_{xc}(\mathbf{r}, \mathbf{r}') \tag{16}$$

Here $\bar{n}(\mathbf{r}, \mathbf{r}')$ is the diagonal part of the two-particle density matrix averaged over λ,

$$\bar{n}(\mathbf{r}, \mathbf{r}') = \int_0^1 d\lambda \; n^{\lambda}(\mathbf{r}, \mathbf{r}') \tag{17}$$

and

$$n^{\lambda}(\mathbf{r}, \mathbf{r}') = < \Psi^{\lambda} | \sum_{i=1}^{N} \sum_{j \neq i}^{N} \delta(\mathbf{r} - \mathbf{r}_i) \delta(\mathbf{r}' - \mathbf{r}_j) | \Psi^{\lambda} > . \tag{18}$$

Integrating (15) over $\mathbf{r}'$ yields

$$E_{xc}[n(\mathbf{r})] = \int d\mathbf{r} \; e_{xc}(n[\mathbf{r}], \mathbf{r}) \tag{19}$$

where e_{xc} is the exchange-correlation energy density derived from the adiabatic connection procedure

$$e_{xc}([n(\mathbf{r})], \mathbf{r}) = \int_0^1 d\lambda \; e_{xc}^{\lambda}([n(\mathbf{r})], \mathbf{r}) \tag{20}$$

with e_{xc}^{λ} given by

$$e_{xc}^{\lambda}([n(\mathbf{r})], \mathbf{r}) = < \Psi_{\lambda} | \frac{1}{2} \sum_{i=1}^{N} \sum_{j \neq i}^{N} \frac{\delta(\mathbf{r} - \mathbf{r}_i)}{|\mathbf{r} - \mathbf{r}_j|} | \Psi_{\lambda} > - \frac{1}{2} \int d\mathbf{r}' \frac{n(\mathbf{r}) n(\mathbf{r}')}{|\mathbf{r} - \mathbf{r}'|} \tag{21}$$

For further reference we note that $n_{xc}^{\lambda=0}$ corresponds to the *density functional* exchange hole n_x. The corresponding excahange energy density is $e_x = e_{xc}^{\lambda=0}$ and the correlation energy density is given by $e_c = e_{xc} - e_x$. Note, however, that the excahnge-correlation energy density, and hence its exchange and

correlation components, are not uniquely defined quantities since we can always add to e_{xc} any function which integartes to zero without affecting the exchange-correlation energy. Our definition of these quantities emerges in a natural way from the adiabatic connection. An alternative definition of the correlation energy density has been suggested by Baerends and Gritsenko (22) and by Huang and Umrigar (23).

3 Quantum Monte Carlo realization

Given an interacting many-body system with ground-state density $n(\mathbf{r})$, the main ingredient for evaluating n_{xc} and e_{xc} is the many-body wavefunction Ψ^{λ} for a number of systems corresponding to different values of the coupling constant λ satisfying the fixed-density constraint. In this section we describe our variational quantum Monte Carlo algorithm for obtaining Ψ_{λ}.

3.1 Variational Monte Carlo

In variational Monte Carlo calculations (7) one starts off with an explicit parameterized *Ansatz* for the ground-state many-body wavefunction of the system under consideration. The total energy of the system is then calculated as the expectation value of the Hamiltonian $\hat{H}$ with respect to the variational wavefunction Ψ_T. Monte Carlo integration is used to perform the multi-dimensional integrals required for evaluating this expectation value and the variational parameters in Ψ_T are adjusted until an optimized wavefunction is obtained. The state-of-the-art method for performing the optimization procedure is the variance minimization scheme (13, 14). In this scheme one minimizes the variance of the local energy $\hat{H}\Psi_T/\Psi_T$ (rather than expectation value of $\hat{H}$) with respect to variational parameters over a set of particle configurations. The use of energy optimized wavefunctions may give unsatisfactory results when quantities other than the energy are evaluated, while minimization of the variance tends to give a better fit for the wavefunction as a whole, so that satisfactory results are obtained for a range of quantities including both energy and electron density. The electron density plays a central role in the adiabatic connection procedure making variance minimization a more suitable choice for optimizing Ψ^{λ}.

3.2 Fixed-density variance minimization

We consider an N-electron system having ground-state density $n(\mathbf{r})$. At a given coupling constant λ the corresponding many-body wavefunction Ψ^{λ} satisfies

equation (10). Therefore, at an arbitrary point $\mathbf{R} = (\mathbf{r}_1, \mathbf{r}_2, \ldots \mathbf{r}_N)$ in the $3N$ dimensional configuration space of electron coordinates, we have

$$\frac{H^\lambda \Psi^\lambda(\mathbf{R})}{\Psi^\lambda(\mathbf{R})} - E^\lambda \equiv 0. \tag{22}$$

In conventional variance minimization calculations (14) (i.e. the unconstrained $\lambda = 1$ case), the above property is used to find an overall fit to Ψ (we drop the λ superscript for simplicity). The procedure is to determine the parameters $\{\alpha\}$ in the trial function $\Psi_T(\mathbf{R}, \{\alpha\})$ by minimizing the variance of local energy σ^2

$$\sigma^2 = \int d\mathbf{R} \left[\frac{H^\lambda \Psi_T(\mathbf{R})}{\Psi_T^\lambda(\mathbf{R})} - E[\Psi_T]\right]^2 |\Psi_T(\mathbf{R})|^2 \tag{23}$$

where $E[\psi_T]$ is the expectation value of the Hamiltonian.

The above unconstrained optimization cannot be directly applied at intermediate values of λ for which the Hamiltonian contains the unknown potential V_λ. We found, however, that a simultaneous determination of Ψ_λ and V_λ can be achieved by performing the following constrained optimization. We assume that the trial many-body wavefunction Ψ_T^λ results in the electron density $n^\lambda(\mathbf{r})$ and expand both $n^\lambda(\mathbf{r})$ and the ground state density $n(\mathbf{r})$ in a complete and orthonormal set of basis functions $\{f_s\}$

$$n(\mathbf{r}) = \sum_{s=1}^{N_d} n_s f_s(\mathbf{r}) \tag{24}$$

$$n^\lambda(\mathbf{r}) = \sum_{s=1}^{N_d} n_s^\lambda f_s(\mathbf{r}) \tag{25}$$

where N_d is a cut-off chosen such that the above expansions converge to $n(\mathbf{r})$ and $n_\lambda(\mathbf{r})$ within a specified accuracy. Subsequently, we define the modified penalty function μ^2

$$\mu^2 = \sigma^2 + W \sum_{s=1}^{N_d} \left[n_s - n_s^\lambda\right]^2 \tag{26}$$

where W is a weight factor the magnitude of which determines the emphasis laid on the fixed-density constraint. The above penalty function reaches its lower bound (of zero) if and only if Ψ^λ is the exact many-body wavefunction satisfying the fixed density constraint (within the accuracy set by N_d) and V^λ is the corresponding exact potential. Hence minimization of μ^2 will, in principle, result in the *simultaneous* determination of Ψ^λ and V^λ. In practice, however, our constrained search is restricted to a sub-space of many-body wavefunctions and minimization of μ^2 yields an optimal fit to Ψ^λ and a corresponding optimal

fit to V^λ, the deviations of which from the exact V^λ reflect the errors in the many-body wavefunction.

Our numerical implementation of the above scheme works as follows. We start off with an initial guesses Ψ_0^λ for the many-body wavefunction and a corresponding guess for V^λ. A fixed number N_c of statistically independent configurations $\mathbf{R}_i$ are then sampled from $|\Psi_0^\lambda|^2$ and the Monte Carlo estimator of μ^2 over these configurations is evaluated

$$\mu^2 = \sum_{i=1}^{N} \left(E_L(\mathbf{R}_i) - < E_L >\right)^2 \left[\frac{\omega_i}{\sum_{j=1}^{N_c} \omega_j}\right] + W \sum_{s=1}^{N_d} [n_s - n_s^\lambda]^2 \tag{27}$$

with

$$E_L(\mathbf{R}_i) = \frac{H\Psi_T^\lambda(\mathbf{R}_i)}{\Psi_T^\lambda(\mathbf{R}_i)} \tag{28}$$

$$\omega_i = \left|\frac{\Psi_T^\lambda}{\Psi_0^\lambda}\right|^2 \tag{29}$$

$< E_L >$ the average energy

$$< E_L >= \sum_{i=1}^{N_c} E_L(\mathbf{R}_i) \left[\frac{\omega_i}{\sum_{j=1}^{N_c} \omega_j}\right] \tag{30}$$

The expansion coefficients of the electron density, n_s^λ, are evaluated from

$$n_s^\lambda = \sum_{i=1}^{N_c} \sum_{k=1}^{N} f^*(\mathbf{r}_k^i) \left[\frac{\omega_i}{\sum_{j=1}^{N_c} \omega_j}\right] \tag{31}$$

where $\mathbf{r}_k^i$ denotes the coordinates of the electron k belonging to configuration i. Finally, we vary the parameters in Ψ_T^λ and V^λ, using a standard NAG routine for optimization, until μ^2 is minimized. We found that setting W equal to the number of configurations results in a satisfactory minimization of both the variance in energy and the error in electron density.

Following (14) we set the reweighting factors ω_i in equations (27) and (30) equal to unity in order to avoid a numerical instability in the variance minimization procedure which occurs for systems with a large number of electrons (these factors, however, are included in calculating the expansion coefficients of the electron density). The above fixed-density variance minimization is then repeated several times until the procedure converges.

4 Cosine-wave jellium

We performed adiabatic connection calculations for the inhomogeneous spin-unpolarized electron gas with average electron density $n_0 = 3/(4\pi r_s^3)$ corresponding to $r_s = 2$. In the QMC simulations we model this system by a finite

system of $N = 64$ electrons satisfying periodic boundary conditions in a FCC simulation cell. Density modulations can be induced by applying an external potential of the form $V_{\mathbf{q}} \cos(\mathbf{q}.\mathbf{r})$ where, because of periodic boundary conditions, $\mathbf{q}$ is restricted to be a reciprocal lattice vector of the simulation cell. Alternatively, we can fix the ground-state electron density *a priori* and use our fixed-density variance minimization method to obtain the corresponding many-body wavefunction at a given Coulomb coupling constant which produces the specified density. In the calculations reported here we chose this second option, with the "target" electron density for the system generated in the following way. We expose the non-interacting electrons (i.e. the $\lambda = 0$ system) to the potential $V(\mathbf{r})$

$$V(\mathbf{r}) = V_{\mathbf{q}} \cos(\mathbf{q}.\mathbf{r}) \tag{32}$$

with $V_{\mathbf{q}} = 2.084\epsilon_F^0$ and $\mathbf{q} = 2\mathbf{B_3}$. Here ϵ_F^0 is the Fermi energy of the unperturbed electron gas, $\mathbf{B_3}$ is a primitive vector of the reciprocal (simulation) cell with $|2\mathbf{B_3}| = 1.11k_F^0$, and k_F^0 is the Fermi wavevector. We then solve the following self-consistent single-particle Schrödinger equations

$$[-\frac{1}{2}\nabla^2 + V_{eff}]\phi_i = \epsilon_i \phi_i \tag{33}$$

with

$$V_{eff}(\mathbf{r}) = V(\mathbf{r}) + V_H(\mathbf{r}) + V_{xc}^{LDA}(\mathbf{r}) \tag{34}$$

to obtain the electron density

$$n(\mathbf{r}) = 2\sum_{i=1}^{N/2} |\phi_i(\mathbf{r})|^2 \tag{35}$$

We *define* this density to be the exact ground-state density of our interacting system. In this way, the single-particle orbitals ϕ_i are by construction the exact Kohn-Sham orbitals and their Slater determinant corresponds exactly to the many-body wavefunction at $\lambda = 0$. Having obtained this non-interacting $v-$representable density we then perform fixed-density variance minimization to produce variational many-body wavefunctions at non-zero Coulomb coupling constants (including the ground-state many-body wavefunction at $\lambda = 1$) which reproduce this density and (variationally) satisfy the Schrödinger equation (10). Once the Ψ_λs are obtained, we use the Monte Carlo Metropolis algorithm to evaluate the required expectation values and perform a numerical coupling constant integration using Gaussian quadrature.

4.1 Many-body wavefunction

The quality of a variational quantum Monte Carlo calculation is determined by the choice of the many-body wavefunction. The many-body wavefunction we use is of the parameterized Slater-Jastrow type which has been shown to yield accurate results both for the homogeneous electron gas and for solid silicon (14) (In the case of silicon, for example, 85% of the fixed-node diffusion Monte Carlo correlation energy is recovered). At a given coupling λ, Ψ^λ is written as

$$\Psi^\lambda = D^\uparrow D^\downarrow \exp\left[-\sum_{i>j} u^\lambda_{\sigma_i,\sigma_j}(r_{ij}) + \sum_i \chi^\lambda(\mathbf{r}_i)\right] \tag{36}$$

where $r_{ij} = |\mathbf{r}_i - \mathbf{r}_j|$ and $D^\uparrow$ and $D^\downarrow$ are Slater determinants of spin-up and spin-down Kohn-Sham orbitals respectively. $u^\lambda_{\sigma_i,\sigma_j}$ is the two-body term correlating the motion of pairs of electrons and σ_i denotes the spin of electron i. Finally, χ^λ is a one-body function which is absent in the homogeneous electron gas but is crucial for a satisfactory description of systems with inhomogeneity. Both u^λ and χ^λ contain variational parameters. We write u^λ as (14)

$$u^\lambda(r) = u^\lambda_0(r) + f^\lambda(r), \tag{37}$$

where u^λ_0 is a fixed function and f^λ is given by

$$\begin{aligned} f^\lambda(r) &= B^\lambda(\tfrac{L_{WS}}{2} + r)(L_{WS} - r)^2 + r^2(L_{WS} - r)^2 \textstyle\sum_{l=0}^{M} \alpha^\lambda_l T_l(\overline{r}) \qquad && 0 \le r \le L_{WS} \\ &= 0 && r > L_{WS} \end{aligned} \tag{38}$$

where B^λ and α^λ_l are variational coefficients, T_l is the lth Chebyshev polynomial, and

$$\overline{r} = \frac{2r - L_{WS}}{L_{WS}}. \tag{39}$$

In the last two equations L_{WS} is the radius of the sphere touching the Wigner-Seitz cell of the simulation cell.

The fixed part of u^λ at full coupling constant $\lambda = 1$ is the short-ranged Yukawa form (14)

$$u^1_0(r) = \frac{A^1}{r}\left(1 - \exp(-\frac{r}{F^1})\right)\exp\left(-\frac{r^2}{L_0^2}\right), \tag{40}$$

where A^1 is fixed by the plasma frequency of the unperturbed electron gas

$$A^1 = \frac{1}{\omega_p^0} \tag{41}$$

and F^1 is fixed by imposing the cusp condition (7) leading to $F^1_{\sigma_i,\sigma_j} = \sqrt{(2A^1)}$ for parallel spins and $F^1_{\sigma_i,\sigma_j} = \sqrt{(A^1)}$ for anti-parallel spins. L_0 is a cut-off parameter chosen so that $u_0(L_{WS})$ is effectively zero and is set equal to $0.25L_{WS}$ in the present calculations. In the case of the unperturbed electron gas, scaling arguments (24) applied to the Hamiltonian (10) result in the following relation for the exact many-body wavefunction at coupling constant λ

$$\Psi^{\lambda}_{r_s}(\mathbf{r}_1, \mathbf{r}_2, \ldots \mathbf{r}_n) = C^{\lambda}\Psi^{\lambda=1}_{r'_s}(\lambda\mathbf{r}_1, \lambda\mathbf{r}_2, \ldots \lambda\mathbf{r}_n) \tag{42}$$

where $\Psi^{\lambda=1}_{r'_s}$ is the ground-state wavefunction of a homogeneous electron gas with the density parameter $r'_s = \lambda r_s$ and C^{λ} is a normalization constant. For the unperturbed electron gas ($\chi \equiv 0$) imposing condition (42) on the fixed-part of our Slater-Jastrow wavefunction yields

$$u^{\lambda}_0(r) = \frac{A^{\lambda}}{r}\left(1 - \exp(-\frac{r}{F^{\lambda}})\right)\exp\left(-\frac{r^2}{L_0^2}\right), \tag{43}$$

where $A^{\lambda} = \lambda^{1/2}A^1$, $F^{\lambda} = \lambda^{-1/4}F^1$. We note that with the above choice for A^{λ} and F^{λ} the $\lambda-$dependent cusp conditions are automatically satisfied. The electron density is modulated only in the $\mathbf{B_3}$ direction and hence both the one-body part of the Jastrow factor and V^{λ} can be expanded as

$$\chi^{\lambda}(\mathbf{r}) = \sum_{m=1}^{M} \chi^{\lambda}(m\mathbf{B_3})\cos(m\mathbf{B_3}.\mathbf{r}) \tag{44}$$

$$V^{\lambda}(\mathbf{r}) = \sum_{m=1}^{M} V^{\lambda}(m\mathbf{B_3})\cos(m\mathbf{B}_3.\mathbf{r}) \tag{45}$$

The electron density is expanded in a similar way (with the inclusion of the $m = 0$ term). We use 7 Fourier coefficients in the expansion of electron density, 6 Fourier coefficients in the expansions of χ_{λ} and V_{λ} (only the first four coefficients turned out to be significantly different from zero), and 8 coefficients (for each of the spin-parallel and spin-antiparallel cases) in the two-body term.

5 Results and discussion

We performed adiabatic connection calculations for cosine-wave jellium using six values of λ: $0, 0.2, 0.4, 0.6, 0.8, 1$. The many-body wavefunctions for $\lambda > 0$ were optimized by fixed-density variance minimization using 10000 independent $N-$electron configurations at each λ. These configurations were regenerated several times. The weight factor in expression (27) was set equal

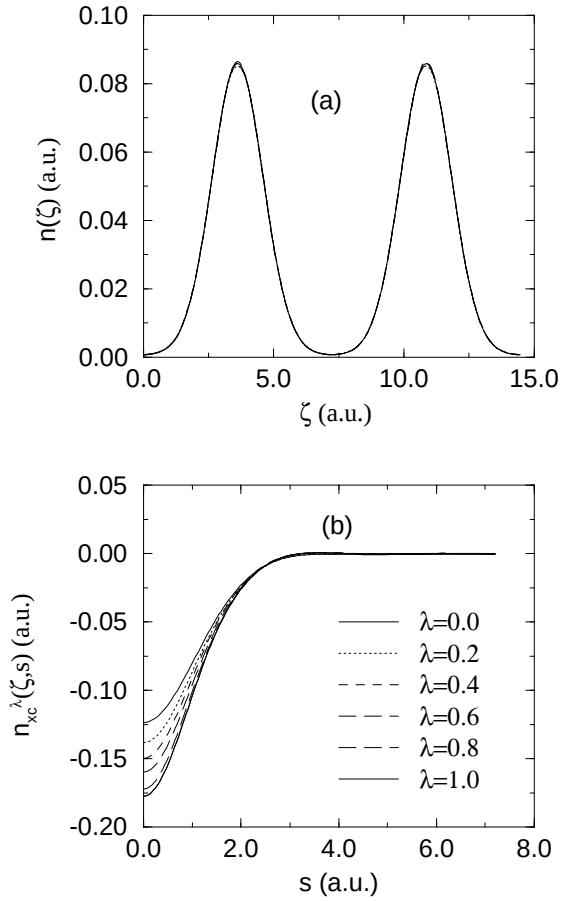

Figure 1: (a) Electron density for different values of λ plotted along ζ (the direction of inhomogeneity). (b) The $\lambda-$dependent spherically averaged exchange-correlation hole for an electron sitting at $\zeta = 10.85$ a.u.

to 10000 in order to obtain a satisfactory minimization of both the variance in energy and the error in electron density. Once Ψ_λ was optimized, quantities of interest were accumulated with the Metropolis Monte Carlo algorithm using 500000 statistically uncorrelated configurations.

We found that our method results in electron densities $n^\lambda(\mathbf{r})$ which deviate from the reference density by less than 1%. This is shown in figure 1(a) where the density is plotted as a function of λ along a line parallel to the direction in which the external potential varies (we call this the ζ direction). While the density is fixed, all other physical quantities vary smoothly and monotically with λ. As an example we consider the spherically-averaged exchange-correlation hole

$$\tilde{n}_{xc}^{\lambda}(\mathbf{r}, s) = \frac{1}{4\pi} \int_{\Omega} d\mathbf{r}' n_{xc}^{\lambda}(\mathbf{r}, \mathbf{r}'), \quad \Omega : |\mathbf{r} - \mathbf{r}'| = s \tag{46}$$

as a function of λ. In figure 1(b) this quantity is shown around an electron sitting at one of the maxima of the electron density ($\zeta = 10.85$ a.u.). The $\lambda = 0$ curve corresponds to the spherically-averaged exchange hole. The ex-

change hole is relatively shallow and negative everywhere. As the interaction is switched on, the hole around the electron becomes gradually deeper. The spherically-averaged hole obeys the sum-rule (3)

$$4\pi \int s^2 \tilde{n}_x^\lambda(\mathbf{r}, s) = -1 \tag{47}$$

and the deepening of the hole for $\lambda > 0$ is compensated by the fact that the hole becomes slightly positive far away from the electron. Note that the hole does not "narrow" as it deepens, but actually broadens. In evaluating $\tilde{\rho}_{xc}^\lambda$ we expanded the exchange-correlation hole in a double Fourier series, sampled the corresponding expansion coefficients and subsequently performed the spherical averaging. Our calculated ρ_{xc}^λ does not satisfy the Kimball cusp-condition (25, 29) because of the finite number of plane-waves in its Fourier expansion. As a result $\tilde{\rho}_{xc}^\lambda$ has zero slope at $s = 0$. We note, however, that this deficiency does not affect E_{xc} and e_{xc}^λ because these quantities are evaluated directly from equations (6) and (21).

Before discussing our findings for this system, we would like to pause and give a short outline of the errors present in our simulations. First of all, the small ($< 1\%$) deviations of the electron density at different λ from the reference density $n(\mathbf{r})$ will induce errors in the adiabatically calculated quantities such as the correlation energy density. By recalculating the exchange energy density with a density which deviates from the reference density by 1% and extrapolating the resulting deviation $e_x[n(\mathbf{r})] - e_x[n(\mathbf{r}) + \delta n(\mathbf{r})]$ to the correlation energy density, we estimate the errors in e_c due to these density deviations to be also $\sim 1\%$.

Further, there are two other kind of errors in our calculations: (i) statistical errors; and (ii) finite size errors (i.e. those caused by the fact that we are using a finite number of electrons to model a supposedly infinite system). With 500000 configurations used in sampling all physical quantities, we found statistical errors to be unimportant, except for the exchange-correlation hole. By evaluating the exchange hole both directly and by Monte Carlo sampling, and assuming that the errors in n_{xc} for $\lambda \neq 0$ are similar, we estimate the statistical error in this quantity to be less than 7%. Another source of errors is finite size effects. These errors occur because a finite simulation cell is used to model an infinite system, with the Coulomb interaction energy evaluated using the Ewald formula (26). The use of a finite simulation cell with periodic boundary conditions affects the wavefunction, of course, and the use of Ewald interaction also produces a Coulomb finite size error in the interaction energy (26, 27). We found the effect of the finite cell on the exchange-correlation hole to be unimportant, except for the asymptotic behavior of this quantity which cannot be correctly described with the present system size. Coulomb finite size

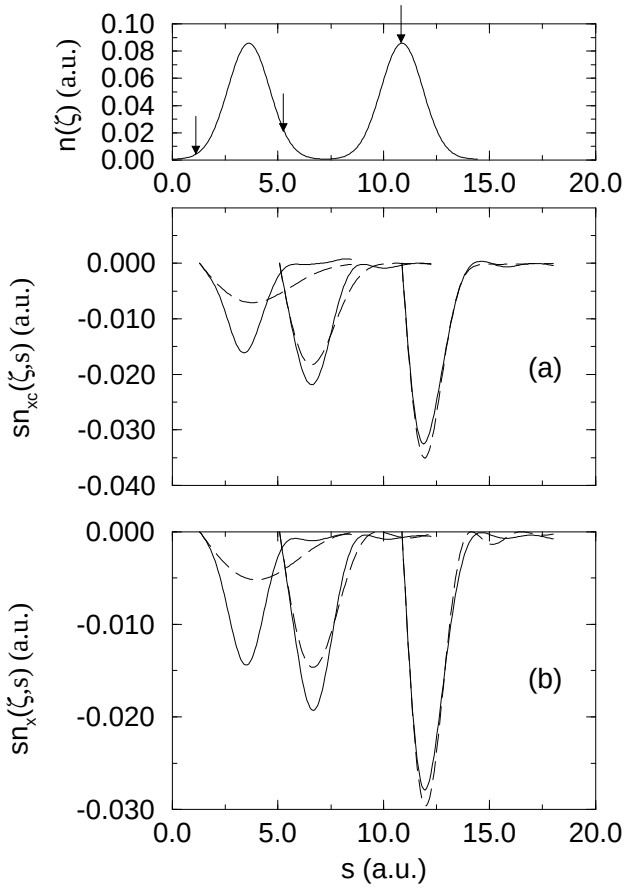

Figure 2: (a) VMC (solid lines) and LDA (dashed lines) $s\tilde{n}_{xc}(\mathbf{r}, s)$ plotted for an electron moving along ζ. Arrows on the electron density (plotted on top), mark the position of the electron. (b) Exact $s\tilde{n}_x(\mathbf{r}, s)$ plotted in the same direction and at the same points as in (a) (solid lines) and the corresponding LDA approximation (dashed lines).

effects do not significantly affect the many-body wavefunctions, and hence their effect on quantities such as the electron density and the exchange-correlation hole is negligible. The exchange-correlation energy density, however, is directly affected by Coulomb finite size effects since in evaluating e_{xc}^{λ} the $1/|\mathbf{r} - \mathbf{r}'|$ Coulomb interaction in (21) is replaced by the periodic Ewald interaction. By calculating the exchange energy density of the homogeneous electron gas using our finite simulation cell and comparing it with the exact result (28)

$$e_x = -\frac{0.45805}{r_s} n_0 \tag{48}$$

we estimate the total finite-size error in e_x to be of the order of -2×10^{-4} a.u; the errors in the correlation energy density e_c is expected to be somewhat

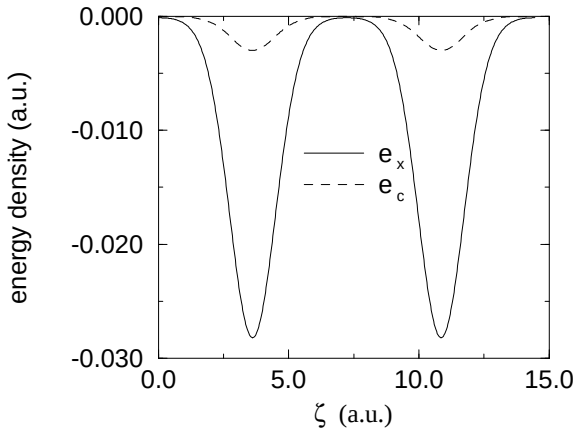

Figure 3: Exchange (solid line) and correlation (dashed line) contributions to e_{xc} plotted along ζ.

smaller.

We now turn to our results for n_{xc} and e_{xc}. The spherically averaged exchange-correlation hole, $\tilde{n}^{\lambda}_{xc}(\mathbf{r}, s)$, obtained from our adiabatic calculations is shown in figure 2(a) together with the LDA approximation (28) to this quantity

$$n^{LDA}_{xc}(\mathbf{r}, s) = n(\mathbf{r})(\bar{g}^{hom}(n(\mathbf{r}), s) - 1) \tag{49}$$

where $\bar{g}^{hom}$ is the λ-averaged pair-correlation function of a homogeneous electron gas with density $n(\mathbf{r})$ (we use the Perdew-Wang parameterization of $\bar{g}$ (29)). In this figure we plot $n_{xc}(\mathbf{r}, s)$ for an electron moving along ζ, and hence fully experiencing the strong variations in electron density. The hole is shown multiplied by s so that the area under each curve is directly proportional to the exchange-correlation energy per electron e_{xc}/n. At $\zeta = 1.30$ a.u. the electron density is very low and n_{xc} is shallow. As electron moves to higher densities ($\zeta = 5.6$ and $\zeta = 10.85$ a.u.) the hole becomes deeper and its asymptotic tail less pronounced. Unlike the LDA hole which depend only on the local density $n(\mathbf{r})$ and is dug out of a homogeneous electron gas of that density, the VMC

hole depends on the density everywhere in the vicinity of $\mathbf{r}$. At $\zeta = 1.30$ a.u, where the electron density is very low, the LDA "probes" only this density and for this reason the LDA exchange-correlation hole is very different from the VMC hole, even close to the electron. As the electron moves to the high density region, the LDA description becomes more satisfactory and at $\zeta = 10.85$ a.u., where the electron density has a maximum, the agreement between the LDA and the VMC hole is rather good. In figure 2(b) we compare the exact exchange hole (obtained from our exact Kohn-Sham orbitals) for the same electron positions with the LDA hole given by (28)

$$\tilde{n}_x^{LDA}(\mathbf{r}, s) = -\frac{9}{2} n(\mathbf{r}) \left[\frac{j_1(k_F(\mathbf{r})s)}{k_F(\mathbf{r})s} \right]^2 , \tag{50}$$

where $k_F(\mathbf{r}) = (3\pi^2 n(\mathbf{r}))^{1/3}$ is the local Fermi wavevector and j_1 the first order spherical Bessel function. Once again, the LDA description is unsatisfactory at low densities but improves as we move to the high density region.

Next we consider exchange-correlation energy densities. In figure 3 the exchange and correlation contributions to this quantity are shown. The differences $e_x^{VMC} - e_x^{LDA}$ and $e_c^{VMC} - e_c^{LDA}$ are shown in figure 4 (a). The difference in e_c follows the variations in electron density and is largest at points where $n(\mathbf{r})$ has a maximum. The differences in e_x shows a more complicated structure and $e_x^{VMC} < e_x^{LDA}$ everywhere in the system. This result is in line with the well-known fact that LDA almost always underestimates the exchange energy of an inhomogeneous system. However, because of the finite size errors, we expect the true e_x to be slightly ($\sim 2 \times 10^{-}4$ a.u.) less negative than e_x^{VMC} so that $e_x < e_x^{LDA}$ must holds in most points of the structure but not necessarily everywhere.

The GGAs for exchange and correlation of a spin-unpolarized system are written as (15)

$$E_x = \int d\mathbf{r}\; n(\mathbf{r}) \epsilon_x^{unif}(n(\mathbf{r})) F_x(s) \tag{51}$$

$$E_c = \int d\mathbf{r}\; n(\mathbf{r}) [\epsilon_c^{unif}(n(\mathbf{r})) + H(n(\mathbf{r}), t)] \tag{52}$$

In the above equations ϵ_x^{unif} and ϵ_c^{unif} are the exchange and correlation energies per particle of a uniform electron gas with density $n(\mathbf{r})$, $t = |\nabla n|/2k_s(\mathbf{r})$, $s = |\nabla n|/2k_F(\mathbf{r})$ with k_s the local Thomas-Fermi wavevector $k_s(\mathbf{r}) = \sqrt{4k_F(\mathbf{r})/\pi}$. In analogy with (19) one may define the GGA e_x and e_c as

$$e_x^{GGA}(\mathbf{r}) = n(\mathbf{r}) \epsilon_x^{unif}(n(\mathbf{r})) F_x(s) \tag{53}$$

and

$$e_c^{GGA}(\mathbf{r}) = n(\mathbf{r}) [\epsilon_c^{unif}(n(\mathbf{r})) + H(n(\mathbf{r}), t)] \tag{54}$$

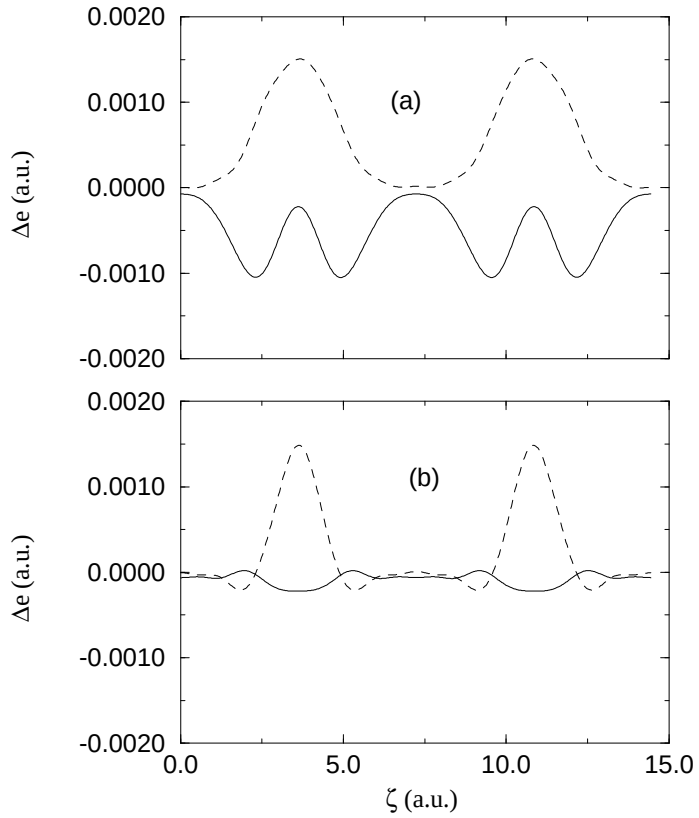

Figure 4: (a) The differences $e_x^{VMC} - e_x^{LDA}$ (solid line) and $e_c^{VMC} - e_c^{LDA}$ (dashed line) plotted along ζ. (b) The same as (a) but for $e_x^{VMC} - e_x^{GGA}$ and $e_c^{VMC} - e_c^{GGA}$.

We note that the above quantities do not directly correspond to the physical e_x and e_c as defined by equation (21) (i.e. via the exchange-correlation hole). Nevertheless, they present pointwise corrections to the LDA exchange and correlation energy densities and for this reason we found it interesting to compare them with our VMC results. In figure 4(b) we show $e_x^{VMC} - e_x^{GGA}$ and $e_c^{VMC} - e_c^{GGA}$. The GGA results were obtained from the ground state density $n(\mathbf{r})$ using the Perdew-Burke-Ernzerhof scheme (15), which we found to give results slightly different from PW91 (6). Note that the difference between the VMC and the GGA exchange energy densities is significantly smaller than that between the VMC and the LDA exchange energy densities, indicating that the GGA improves upon the LDA in describing this quantity. As for e_c, the differences are of the same order as for the LDA, although the shape is

different. It is interesting that the LDA errors in e_x and e_c partially cancel each other, even on a local scale, but that these cancellations do not occur for the GGA. In summary, the GGA seems to do a good job in improving the LDA description of the exchange energy density but is less successful in the case of the correlation energy density. The resulting exchange correlation energy per electron obtained from VMC, LDA and GGA are $E_{xc}^{VMC}/N = -0.328 \pm 0.009$, $E_{xc}^{LDA}/N = -0.3296$, $E_{xc}^{GGA}/N = -0.3347$ a.u.

Acknowledgments

We thank Randy Hood and Mei-Yin Chou for helpful discussions. Part of this work has been supported by the Human Capital and Mobility Program through contract No. CHRX-CT94-0462.

References

(1) P. Hohenberg and W. Kohn, Phys. Rev. **136**, B864 (1964).

(2) W. Kohn and L.J. Sham, Phys. Rev. **140**, A1133 (1965).

(3) R.G. Parr and W. Yang, *Density Functional Theory of Atoms and Molecules* (Oxford University Press, New York, 1989).

(4) D.C. Langreth and M.J. Mehl, Phys. Rev. B **28**, 1809 (1983).

(5) A.D. Becke, Phys. Rev. A **38**, 3098 (1988).

(6) J.P. Perdew *et al.*, Phys. Rev. B **46**, 6671 (1992); **48**, 4978 (1993) (E).

(7) B.L. Hammond, W.A. Lester, Jr. and R.J. Reynolds, *Monte Carlo Methods in Ab Initio Quantum Chemistry* (World Scientific, Singapore, 1994).

(8) C.J. Umrigar and X. Gonze in *High Performance Computing and its Applications to the Physical Science*, edited by D.A. Browne *et al.* (World Scientific, Singapore, 1993).

(9) C. Filippi, C.J. Umrigar and X. Gonze, Phys. Rev. A **54**, 4810 (1996).

(10) W. Knorr and R.W. Godby, Phys. Rev. Lett. **68**, 639 (1992).

(11) G.E. Engel, Y. Kwon and R.M. Martin, Phys Rev. B **51** (1995).

(12) R.Q. Hood *et al.* Phys. Rev. Lett. **78**, 3350 (1997).

(13) C.J. Umrigar, K.G. Wilson and J.W. Wilkins, Phys. Rev. Lett. **60**, 1719 (1988).

(14) A.J. Williamson *et al.*, Phys. Rev. B **53**, 9640 (1996).

(15) J.P. Perdew, K. Burke and M. Ernzerhof, Phys. Rev. Lett. **77**, 3865 (1996).

(16) J. Harris and R.O. Jones, J. Phys. F **4**, 1170 (1974).

(17) D.C. Langreth and J.P. Perdew, Phys. Rev. B **21**, 5469 (1980).

(18) O. Gunnarson and B.I. Lundqvist, Phys. Rev. B **13**, 4274 (1976).

(19) M. Levy in *Density Functional Theory*, edited by J. Keller and J.L. Gasquez (Springer, New york, 1983).

(20) E.H. Lieb, in *Physics as Natural Philosophy*, edited by A. Shimony, H. Feshbach (MIT Press, Cambridge, Mas, 1982).

(21) H. Englisch and R. Englisch, Physica (Utrecht) **21A**, 253 (1983).

(22) E.J. Baerends and O.V. Gritsenko J. Phys. Chem., **101**, 5383 (1997).

(23) Chien-Juang Huang and C.J. Umrigar, Phys. Rev. A, **56**, 290 (1997).

(24) M. Levy and J.P. Perdew, Phys. Rev. A **32**, 2010 (1985).

(25) A.K. Rajagopal, J.C. Kimball and M. Banerjee, Phys. Rev. B **18**, 2339 (1978); J.C. Kimball, Phys. Rev. A **7**, 1648 (1973).

(26) L.M. Fraser *et al.*, Phys. Rev. B **53**, 1814 (1996).

(27) A.J. Williamson *et al.*, Phys. Rev. B **55**, R4851 (1997).

(28) R.M. Dreizler and E.K.U. Gross, *Density Functional Theory, An approach to the Quantum Many-Body Problem*, (Springer-Verlag, Berlin 1990).

(29) J.P. Perdew and Y. Wang, Phys. Rev. B **46**, 12947 (1992).

(30) J.P. Perdew and K. Burke, private communication.